Accepted Manuscript

Synthesis of 4-aminoquinoline–pyrimidine hybrids as potent antimalarials and their mode of action studies

Kamaljit Singh, Hardeep Kaur, Kelly Chibale, Jan Balzarini

PII: S0223-5234(13)00364-4

DOI: 10.1016/j.ejmech.2013.05.046

Reference: EJMECH 6224

To appear in: *European Journal of Medicinal Chemistry*

Received Date: 6 May 2013

Revised Date: 29 May 2013

Accepted Date: 30 May 2013

Please cite this article as: K. Singh, H. Kaur, K. Chibale, J. Balzarini, Synthesis of 4-aminoquinoline–pyrimidine hybrids as potent antimalarials and their mode of action studies, *European Journal of Medicinal Chemistry* (2013), doi: 10.1016/j.ejmech.2013.05.046.

Graphical Abstract

Synthesis of 4-aminoquinoline–pyrimidine hybrids as potent antimalarials and their mode of action studies

Kamaljit Singh, Hardeep Kaur, Kelly Chibale, and Jan Balzarini

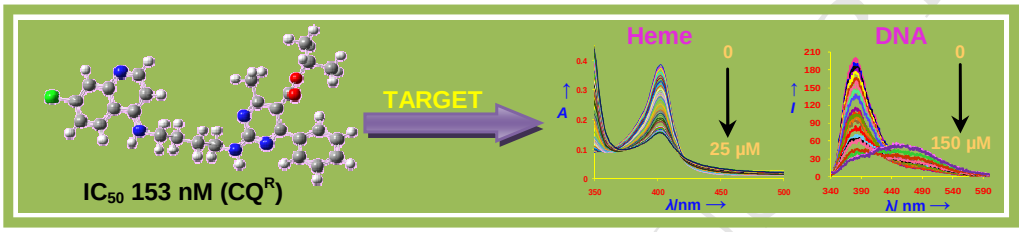

Efficaciously synthesized new 4-aminoquinoline-pyrimidine hybrids depict antiplasmodial activity (nM) against CQ^R and CQ^S strains of *Plasmidum falciparum*. Representative compounds revealed binding with heme and AT rich pUC18 DNA, spectrophotometically.

Synthesis of 4-aminoquinoline–pyrimidine hybrids as potent antimalarials and their mode of action studies

Kamaljit Singh,[a,*] Hardeep Kaur,[a] Kelly Chibale,[b] and Jan Balzarini[c]

[a]Department of Chemistry, UGC-Centre of Advance Study-1, Guru Nanak Dev University, Amritsar – 143005, India[♣]

[b]Department of Chemistry and Institute of Infectious Disease and Molecular Medicine, University of Cape Town, Rondebosch 701, South Africa

[c]Rega Institute for Medical Research, Katholieke University Leuven, 10 Minderbroedersstraat, B-3000 Leuven, Belgium

Abstract: One of the most viable options to tackle the growing resistance to the antimalarial drugs such as artemisinin is to resort to synthetic drugs. The multi-target strategy involving the use of hybrid drugs has shown promise. In line with this, new hybrids of quinoline with pyrimidine have been synthesized and evaluated for their antiplasmodial activity against both CQ^S and CQ^R strains of *Plasmodium falciparum*. These depicted activity in nanomolar range and were found to bind to heme as well as AT rich pUC18 DNA.

Keywords- Antimalarials; 4-aminoquinolines; heme binding; hybrid molecules; drug discovery.

1. Introduction

Malaria is one of the most widespread diseases besides tuberculosis and AIDS which affects more than 500 million people worldwide and results in around 1–3 million causalities every year [1]. In Africa alone, around 20% childhood deaths are due to malaria and a child dies every 30s [2] and it is estimated that an African child has on an average 1.6 to 5.4 episodes of

♣ Corresponding author. Tel.: +91 183 2258853; Fax: +91 183 2258819-20. E-mail address: kamaljit19in@yahoo.co.in *(Kamaljit Singh).*

malaria fever each year. Of the four typically recognized *Plasmodium* species causing disease in humans, *Plasmodium falciparum* is most deadly to children below the age of five leading to mortality while *Plasmodium vivax* is most morbidity prone, and is responsible for latent infection that hampers current control and future elimination efforts [3]. The development of drug resistance for the common antimalarials such as 4-/8-aminoquinolines, 4-methanol quinolines, antifolate drugs, sesquiterpene lactones etc. (Figure 1) is a rather serious issue which has stimulated considerable research efforts in the development of new drugs using different approaches [4,5] of which the molecular hybridization approach [6,7] is quite an attractive strategy which involves design of new chemical entities by covalent fusion of two drugs, both active compounds and/or pharmacophoric units derived from known bioactive molecules with complimentary activities and multiple pharmacological targets. The multiple target strategy led to the design of hybrid of 4-aminoquinoline with species such as triazine [8,9], ferrocene [10], rhodanine [11], thiazolidine-4-one [12], chalcone [13], trioxane [14], isatin [15] and recently, pyrimidines [16-18] (Figure 2).

Insert Figure 1 here

Quinoline containing drugs (chloroquine and primaquine, Figure 1) are known to affect parasite metabolism and cause parasite death by blocking the polymerization of the toxic heme, into an insoluble and non-toxic pigment, hemozoin, resulting in cell lysis and parasite cell auto digestion [19-21]. On the other hand, pyrimidine-based compounds are well known for their wide range of promising antiviral [22] , antitubercular [23], anti-AIDS [24], antinociceptive [25], antifungal [26], antitumor [27]and antimalarial activities [28] apart from their role in the nucleic acid synthesis. Thus, linking of the quinoline unit with pyrimidine might furnish conjugate hybrids that are capable of showing useful antimalarial activity.

Insert Figure 2 here

Recently, antimalarial activities of some quinoline-pyrimidine hybrids with activities in the micromolar to nanomolar range have been reported (Figure 3) [16-18,29]. In yet another report on the evaluation of quinoline-pyrimidine, the activity (in micromolar range) was also reported for fixed combinations of the chloroquine and pyrimethamine. In all these reports, the pyrimidines were linked to the quinoline unit through 2-, 4- and 6- positions. We have employed rather conformationally flexible pyrimidine-5-carboxylates linked covalently to 4-

aminoquinoline core. These novel pyrimidine carboxylate hybrids interact with the iron center of free heme within the physiological environment (pH 5.6), a key step in the accumulation of heme which is selectively toxic to the parasite. To enhance the possibility to accumulate within the digestive vacuole *via* weak-base trapping (the mechanism by which CQ and other quinoline antimalarials attain high concentrations inside this compartment), we developed a novel class of antimalarials using a pharmacophore hybridization approach in which the pyrimidine-5-carboxylate motif was hybridized with an iron-complexing, 4-aminoquinoline moiety through C-2 position [29]. To further elaborate the structure-activity profile, here, we present additional new 4-aminoquinoline-pyrimidine carboxylate hybrids. We also report on their antimalarial activity against both CQ sensitive (CQ^S Dd2) as well as CQ resistant (CQ^R D10) strains. Finally, the mechanism of action studies with the representative compounds has also been performed.

Insert here Figure 3

2. Chemistry

The 4-aminoquinoline-pyrimidine-5-carboxylate hybrids were synthesized in economical way using synthetic approach outlined in Scheme 1. The key starting compound, 3,4-dihydropyrimidin-2(1H)-one **1** was prepared through NH_4Cl/TFA [30,31] catalyzed three-component Biginelli condensation of an alkyl acetoacetate, urea and appropriate aldehyde or its formyl equivalent: 1,3-oxazinane derivative, in acetonitrile or under solvent-free reaction conditions, in some cases. Subsequent oxidation of **1** using 60% nitric acid readily furnished pyrimidinones **2** which upon chlorination with $POCl_3$ yielded **3 [**32]. The nucleophilic substitution reaction of **3** with appropriate 4-amino-7-chloroquinoline **4** which in turn was prepared from the commercially available 4,7-dichloroquinoline and diaminoalkanes [33], gave **5a-g** in good yields (Table 1). Structures of **1**-**5** were unambiguously established on the basis of spectral (^{1}H NMR, ^{13}C NMR, MS, FT IR) as well as microanalytical analysis.

Insert here Scheme 1.

3. Results and Discussion

3.1. Antimalarial activity and structure-activity relationships (SARs)

We have previously established that the 4-aminoquinoline-pyrimidine hybrids **6a-c** intercepted by a diaminoalkyl spacer showed optimum potency (Table 1), when the flexible spacer consisted of three or four carbon atoms [29]. Further, the introduction of nitro substituent at ortho position of the phenyl ring at the C-4 of the pyrimidine core furnished the most potent compound **6c** with antimalarial activity superior to the standard CQ and close to artesunate [29]. Keeping these observations in mind, we planned to further refine the activity of these persuasive 4-aminoquinoline-pyrimidine by incorporating electron withdrawing substituents at C-4 phenyl of pyrimidine core, as well as by varying the C-5 ester substituent and also by altering the basicity of diaminoalkyl spacer.

Insert Table 1 here

The *in vitro* antimalarial screening of the new synthesized compounds **5a-g** revealed good to moderate activities in nM range against both the tested Dd2 (CQ^S) and D10 strains (CQ^R) of *P. falciparum* (Table 1). Although the tested hybrids were not as active as the standard drugs *viz.* CQ and ASN, interesting SARs have been drawn. Analysis of the activity of the compounds recorded in Table 1 reveals that replacing C-5 ethyl ester of the previously reported [29] compound **6a** [IC_{50} 247.5 nM (CQ^S); 52.2 nM (CQ^R)] with methyl ester **5a** [IC_{50} 659 nM (CQ^S); 542 nM (CQ^R)] led to the decrease in antimalarial activity against both the chloroquine sensitive and chloroquine resistant strains of *P. falciparum*. However, comparison of hybrids **5b**, **5c** with **6b**, **6c** having an identical butyl spacer showed that incorporation of isopropyl ester at C-5 of pyrimidine motif (**5b** and **6b)** increased the antimalarial activity against the CQ^S strain whereas considerable decrease in activity was observed for CQ^R strain of *P. falciparum*. Also, the most potent compound **5b** of the series displayed 2-fold increase in antimalarial activity than the standard CQ against CQ^R strain of *P. falciparum*. When the diaminoalkyl linker of compound **6a** was replaced with relatively less basic alkoxy amino linker **5d** considerable decrease in antimalarial activity was observed which in turn linked to the decreased accumulation of compound *via* pH trapping into the digestive vacuole. It was not unexpected since the basicity of alkyl chain linker plays crucial role in determining the antimalarial activity of this class of compounds. Furthermore, the introduction of a nitro substituent on the phenyl ring at the C-4 position of the pyrimidine core to create **5c** resulted in a significant increase in anti-plasmodial activity in comparison to the p-chloro/p-fluoro substituents (**5e** and **5f**). Moreover, the hybrid **5g**

lacking a C-4 substituent on the pyrimidine motif led to an increase in antimalarial activity against both the CQ^S as well as CQ^R strains of *P. falciparum*. However, although the antimalarial activity of **5g** was superior to **5c**, **5e** & **5f**, it was less than the corresponding C-4 phenyl substituted analogues **5b** as well as **6b**.

Thus, the SAR study suggested that both the substitution of the C-4 phenyl group with electron withdrawing groups and alterations in basicity of linker leads to better antimalarial activity. Unfortunately, these compounds suffer from high ClogP values which are in the range 5-8 (Table 1), which are suggestive of the fact that these possess limited aqueous solubility. However, it is not a serious limitation in view of recent advancements in formulation methods.

3.2. Cytotoxicity and antiviral activity

Compounds **5a-g** were evaluated for their toxicity against various (Hela, Vero, CRFK, Hel and MDCK) cell cultures (Table 1 & SI Table S1). Toxicity data revealed that these compounds exhibit high toxicity against MDCK cell cultures while toxicity concentrations are quiet high for other cell cultures. The CC_{50} values for inhibition of MDCK cells summarized in Table 1 indicate that the strongest antimalarial compound **5b** was mildly cytotoxic (Table 1). Further, the ratio of the cytotoxicity (CC_{50} in μM) and in vitro antimalarial activity (IC_{50} in nM for Dd2 strain) enabled the determination of selectivity index (SI) for these compounds. Compound **5d** with alkoxy amino linker and compound **5g** bearing C-4 unsubstituted pyrimidine motif exhibited high toxicity concentrations (CC_{50}) and thus led to the fairly safe selectivity index values (Table 1). Compound **5d** having less basic alkyl spacer, displayed highest SI (43.6) whereas the most potent compound **5b** exhibit relatively low SI value (3.92). Thus, the compounds depicted structure dependent SI values.

Chloroquine is known to elicit antiviral effects against several viruses, including human immunodeficiency virus type 1, HCoV-229E, hepatitis B virus, and herpes simplex virus type 1 [34-37]. Thus, we determined in vitro antiviral activities of **5a-g** against (i) herpes simplex virus-1 (HSV-1; KOS), herpes simplex virus-2 (HSV-2; G), vaccinia virus, vesicular stomatitis virus, herpes simplex virus-1 (TK^-KOS ACVR) in HEL cell cultures, (ii) parainfluenza-3 virus, reovirus-1, Sindbis virus, Coxsackie virus B4, Punta Toro virus in vero cell cultures, (iii) influenza A virus (H1N1 and H3N2) and influenza B virus in MDCK cell cultures, (iv) vesicular stomatitis virus, coxsackie virus B4, respiratory syncytialvirus in HeLa cell cultures, (v)

cytomegalovirus using AD-169 and Davis strain in HeL cells, (vi) varicella-zoster virus (VZV) in HeL cells (SI Table S1) and (vii) felinecorona virus (FIPV) and feline herpes virus activity in CRFK cell cultures (Table 2). The anti-viral activity of most of the compounds was not impressive except compounds **5a** and **5c** which exhibited relatively low MICs only against the feline corona virus (FIPV) and feline herpes virus in CRFK cell cultures (Table 2).

Insert here Table 2

3.3. Mode of action studies

3.3.1. Heme binding studies

Quinoline antimalarials (e.g., CQ, amodiaquine and quinine) act principally by forming adducts with ferriprotoporphyrin IX, thus blocking haemozoin formation [38]. In this study, we have evaluated the mechanism of antimalarial activity of the most potent compound **5b** of the series by studying its binding with heme [Fe(III)PPIX] in solution and inhibition of β-hematin formation using UV-visible spectrophotometer. The incremental addition of **5b** (0-25 μM) into monomeric heme (2.4 μM, DMSO:H_2O/4:6, *v/v*) in 0.02 M HEPES buffer (pH 7.4) showed a substantial decrease in the intensity of the Fe(III) PPIX Soret band at 402 nm with no shift in the wavelength of the absorption maximum (Figure 4). The titration of monomeric heme was also performed at the *Plasmodial* food vacuole pH 5.6 using MES buffer instead of HEPES to ensure that the compound **5b** binds with heme even at acidic pH (S1†). A 1:1 stoichiometry of the most stable complex of **5b** with monomeric heme at pH 7.4 and 5.6 was established from the Job's plot (SI Figure S1).The association constants (Table 3) were calculated by analyzing the titration curves obtained at pH 7.4 using HypSpec-a non-linear least square fitting programme [39]. The binding of CQ with heme under identical conditions was also determined in the similar manner and the results are presented in Table 3 for comparison. Table 3 shows that the association constants for the complexes formed between monomeric heme and **5b** (log *K* 4.96) are comparable with those of standard antimalarial drug, CQ (log *K* 5.15). Furthermore, the decrease of apparent pH from 7.4 to 5.6 (Table 3) has little effect on the binding constants indicating binding is stronger even at acidic pH.

Insert here Figure 4

Insert here Table 3

To further establish the binding of **5b** with monomeric heme, ^{1}H NMR titrations were performed and shifts in the peaks as well as peak intensity noted. The addition of 30 mol% of heme dissolved in 40% DMSO to a solution of **5b** in 40% DMSO:D_2O\D_2SO_4 (10 µl) caused a shift in the aromatic proton signals (Figure 5), indicating binding of **5b** with heme but further addition of heme led to broadening of the peaks. An equimolar (3.9 µmol) solution of hemin chloride and **5b** when analyzed in mass spectrometer depicted an intense molecular ion peak at 1119.3769 Da (Figure 6a), corresponding to the molecular formula $C_{62}H_{62}ClFeN_9O_6$, suggesting the formation of 1:1 complex. Thus, we propose that **5b** interact with heme by replacing chloride atom of hemin chloride and coordinating the iron atom with its endocyclic quinoline nitrogen as proposed in Figure 6b.

Insert Figure 5 and Figure 6 here

Similar titration of dimers of µ-oxo type (10 µM) at pH 5.8 using standard procedure [29] with increasing concentration of compound **5b** (0-14 µM), resulted in decrease in intensity of broad peak at 362 nm (Figure 7a, S1†). Further, Job's plot calculations indicated a 1:1stoichiometry for the most stable µ-oxo: **5b** complex (Figure 7b). In Table 3 the association constants of **5b** (log *K* 5.72) are compared to that of standard CQ (log *K* 5.58) and also suggests that the binding of **5b** is stronger with µ-oxoheme (log *K* 5.72) than monomeric heme (log *K* 4.96). Thus, the compound **5b** inhibit hemozoin formation by blocking the growing face of heme resulting in the observed antimalarial activity. Furthermore, the β-hematin inhibition assay (SI Table S2) shows that there is no correlation between antimalarial activity and β-hematin inhibition and also, all the compounds inhibit β-hematin formation although less than that of standard CQ.

Insert Figure 7 here

3.3.2. DNA binding studies

The mechanism of many antimalarial drugs such as CQ, quinacrine and quinine relies upon the interaction with DNA presumably through ionic interactions between phosphate groups of DNA and protonated amine in addition to the interactions between aromatic nuclei of the drug with nucleotide bases [40,41]. Therefore, the DNA binding properties of 4-aminoquinoline-pyrimidine hybrids have been evaluated using both the UV-visible spectrophotometer and

fluorescence spectrophotometry in order to probe interaction of these compounds with DNA. The addition of CT-DNA (4-200 µM) to the buffered methanolic solution of **5b** (30 µM) induced hyperchromic shift of 112% in absorption band at 255 nm whereas hypochromic shift of 37% in the characteristic quinoline ring absorption at 330 nm (Figure 8). Also, the bathochromic shift of ~3 nm was observed for both the absorptions. The observed hyperchromic as well as hypochromic shifts in absorption bands of **5b** upon addition of DNA results from the intercalation of **5b** with CT DNA as suggested in the literature [42]. The intercalative nature of interaction of compound **5b** with CT DNA was additionally supported by thermal denaturation experiment. Intercalation of molecules into the double helix is known to stabilize the DNA against thermal strand separation and thus increases thermal melting temperature (T_m) [43,44]. The derivative melting curve presented in Figure 9 shows an increase of 7.5 ºC in thermal melting temperature of CT DNA upon addition of **5b** which is less than that observed for the CQ (Table S3). Thus, both the UV-visible titrations and thermal denaturation experiment advocate partial intercalative nature of interactions between compound **5b** and CT DNA.

Insert Figure 8 and Figure 9 here

Further, to visualize the effect of DNA base composition, the fluorescence titrations of **5b** were performed with both GC-rich CT DNA and AT-rich pUC18 DNA in buffered methanol. Figure 10 shows decrease in the intensity of the emission band of **5b** at 380 nm, upon addition of increasing concentration of both the DNAs. A shift of 80 nm in emission band at 380 nm was observed upon addition of CT DNA but no such shift inemission band was observed for pUC 18 DNA. Comparison of binding constant of **5b** with CT DNA (log *K* 5.76) and pUC 18 DNA (log *K* 5.73) calculated from titration data using HypSpec [39], suggest that **5b** does not discriminate between GC rich DNA and AT rich DNA.

Insert Figure 10 here

4. Conclusions

A series of potent 4-aminoquinoline-pyrimidine hybrids with antimalarial activity in nano molar range were reported. The compound **5b** exhibit lowest IC_{50} value within the series against both CQ^S and CQ^R strains of *P. falciparum*. These hybrids displayed mild toxicity against MDCK cell cultures. The antiviral activity profiles of these hybrids indicate that the compound

5a and **5c** effectively inhibit feline corona virus and feline herpes virus. Further, the mechanism of observed antimalarial activity was established in terms of binding with heme as well as DNA.

5. Experimental

5.1. General

All liquid reagents were dried/purified following recommended drying agents and/or distilled over 4 Å molecular sieves. THF was dried (Na- benzophenone ketyl) under nitrogen. ^{1}H NMR (300 MHz) and ^{13}C (75 MHz) NMR spectra were recorded in $CDCl_3$ on a multinuclear Jeol FT-AL-300 spectrometer with chemical shifts being reported in parts per million (δ) relative to internal tetramethylsilane (TMS, δ 0.0, ^{1}H NMR) or chloroform ($CDCl_3$, δ77.0, ^{13}C NMR). Mass spectra were recorded at Department of Chemistry, Guru Nanak Dev University, Amritsar on a Bruker LC-MS MICROTOF II spectrometer. Elemental analysis was performed on FLASH EA 112 (Thermo electron Corporation) analyzer at Department of Chemistry, Guru Nanak Dev University, Amritsar and the results are quoted in %. IR spectra were recorded on Perkin Elmer FTIR-C92035 Fourier transform spectrometer in the range 400-4000 cm^{-1}using KBr pellets. Melting points were determined in open capillaries and are uncorrected. For monitoring the progress of a reaction and for comparison purpose, thin layer chromatography (TLC) was performed on pre-coated aluminum sheets of Merck ($60F_{254}$, 0.2 mm) using an appropriate solvent system. The chromatograms were visualized under UV light. For column chromatography silica gel (60-120 mesh) was employed and eluents were ethyl acetate/hexane or ethyl acetate/methanol mixtures. The steady state fluorescence experiments were carried out on Perkin Elmer LS55 fluorescence spectrometer at ambient temperature. UV-visible spectral studies were conducted on Shimadzu 1601 PC spectrophotometer with a quartz cuvette (path length, 1 cm). The absorption spectra have been recorded between 1100 and 200 nm. The cell holder of the spectrophotometer was thermostatted at 25°C for consistency in the recordings.

5.2. General procedure for synthesis of **5a** and **5b**

To the stirred solution of **3** (2 mmol) and potassium carbonate (5 mmol) in dry THF (30 ml), a solution of appropriate 4-aminoquinoline **4** (1.0 mmol) in dry THF (50 ml) was added. The reaction mixture was stirred for 48 h at room temperature. The reaction mixture was filtered and THF was removed under vacuum. The residue was purified by column chromatography

using MeOH/ethyl acetate as eluent to obtain corresponding **5**, which was recrystallized from DCM/ hexane. Using this procedure the following compounds were isolated.

5.2.1. Methyl 2-(3-((7-chloroquinolin-4-yl)amino)propylamino)-4-methyl-6-phenylpyrimidine-5-carboxylate (**5a**). White solid. Rf: 0.47 (4% MeOH/ethyl acetate). Yield: 86%. m.p.105ºC. IR (KBr): ν_{max} 770, 1267, 1709, 2928, 3427 cm^{-1}. ^1H NMR (300 MHz, $CDCl_3$, 25°C): δ 2.00 (q, *J* = 6.3 Hz, 2H, CH_2), 2.49 (s, 3H, C6-CH_3), 3.46 (m, 2H, CH_2), 3.58 (s, 3H, ester-CH_3), 3.68 (q, *J* = 6.6 Hz, 2H, CH_2), 5.57 (br, 1H, NH), 6.41 (d, 1H, ArH), 6.44 (br, 1H, NH), 7.39-7.54 (m, 7H, ArH), 7.91 (s, 1H, ArH), 8.48 (d, 1H, ArH). ^{13}C NMR (75 MHz, $CDCl_3$, 25°C): δ 14.8, 20.6, 30.0, 31.6, 43.8, 90.6, 92.3, 112.7, 116.8, 119.5, 120.2, 121.5, 126.5, 141.3, 143.6, 153.5, 159.1, 160.8. Anal. Calcd. for $C_{25}H_{24}N_5O_2Cl$: C, 65.00; H, 5.24; N, 15.10; Found: C, 65.14; H, 5.19; N, 14.99. MS: *m/z* 462 [M^+].

5.2.2. *i*-Propyl 2-(4-((7-chloroquinolin-4-yl)amino)butylamino)-4-methyl-6-phenylpyrimidine-5-carboxylate (**5b**). White solid. Rf: 0.41 (4% MeOH/ethyl acetate). Yield: 83%. m.p. 140ºC. IR (KBr): ν_{max} 1368, 1724, 2993, 3473 cm^{-1}. ^1H NMR (400 MHz, $CDCl_3$, 25°C): δ 1.0 (d, *J* = 5.6 Hz, 6H, 2×ester-CH_3), 1.78 (m, 4H, CH_2), 2.46 (s, 3H, C6-CH_3), 3.33 (m, 2H, CH_2), 3.50 (m, 2H, CH_2), 4.99 (m, 1H, ester-CH), 5.44 (br, 1H, NH), 5.67 (br, 1H, NH), 6.34 (d, *J* = 5.3 Hz, 1H, ArH), 7.27-7.63 (m, 7H, ArH), 7.93 (d, *J* = 1.4 Hz, 1H, ArH), 8.46 (d, *J* = 5.3 Hz, 1H, ArH). ^{13}C NMR (75 MHz, $CDCl_3$, 25°C): δ 21.3, 22.9, 25.8, 27.4, 40.7, 42.9, 68.9, 98.9, 116.0, 117.0, 121.3, 125.3, 129.5, 135.0, 138.9, 148.4, 150.0, 151.3, 161.2, 165.8, 166.9, 168.3. Anal. Calcd. For $C_{28}H_{30}N_5O_2Cl$: C, 66.72; H, 6.00; N, 13.89; Found: C, 66.50; H, 5.88; N, 13.65. MS: *m/z* 503.2 [M^+].

5.3. General procedure for the synthesis of compound **5c-g**

To the stirred solution of appropriate 4-aminoquinoline **4** in dry acetonitrile (50 ml) mixture of **3** (in a 1:2 molar ratio) and potassium carbonate in dry acetonitrile was added. The reaction mixture was refluxed for 24 h and then filtered. Acetonitrile was removed under vacuum and the residue was purified by column chromatography using MeOH/ethyl acetate as eluent to give **5** which is recrystallized from DCM/ hexane.

5.3.1. Ethyl 2-(4-((7-chloroquinolin-4-yl)amino)butylamino)-4-methyl-6-(2-nitrophenyl)pyrimidine-5-carboxylate (**5c**). Yellow solid. Rf: 0.28 (4% MeOH/ethyl acetate). Yield: 75%. m.p. 72ºC. IR (KBr): ν_{max} 769, 1550, 1355, 1720, 2930, 3365 cm^{-1}. ^1H NMR (400

MHz, $CDCl_3$, 25°C): δ 0.87 (t, *J* = 7.1 Hz, 3H, ester-CH_3), 1.76 (m, 4H, CH_2), 2.57 (s, 3H, C6-CH_3), 3.27 (m, 2H, CH_2), 3.47 (m, 2H, CH_2), 3.96 (q, *J* = 7.0 Hz, 2H, ester-CH_2), 6.07 (br, 1H, NH), 6.26 (d, *J* = 4.8 Hz, 1H, ArH), 6.33 (br, 1H, NH), 7.22-7.86 (m, 6H, ArH), 8.11 (s,1H, ArH), 8.32 (d, *J* = 5.4 Hz, 1H, ArH). ^{13}C NMR (100 MHz, $CDCl_3$, 25°C): δ 12.5, 22.1, 24.4, 28.6, 39.7, 42.2, 59.7, 97.4, 115.6, 121.3, 123.2, 124.5, 125.0, 128.2, 128.6, 131.9, 134.7, 145.2, 148.3, 150.1, 159.9, 165.3, 176.3. Anal. Calcd. For $C_{27}H_{27}N_6O_4Cl$: C, 60.62; H, 5.09; N, 15.7; Found: C, 60.34; H, 5.01; N, 15.58. MS: *m/z* 534.2 [M^+].

5.3.2. Ethyl 2-(3-((7-chloroquinolin-4-yl)amino)propoxy)-4-methyl-6-phenylpyrimidine-5-carboxylate (**5d**). White solid. Rf: 0.38 (4% MeOH/ethyl acetate). Yield: 90%. m.p.110ºC. IR (KBr): ν_{max} 1255, 1775, 2969, 3530 cm^{-1}. ^{1}H NMR (300 MHz, $CDCl_3$, 25°C): δ 1.05 (t, *J* = 7.2 Hz, 3H, ester-CH_3), 2.43 (m, 2H, CH_2), 2.59 (s, 3H, C6-CH_3), 3.56 (m, 2H, CH_2), 4.13 (t, *J* = 7.2 Hz, 2H, CH_2), 4.68 (q, *J* = 6.0 Hz, 2H, ester-CH_2), 5.70 (br, 1H, NH), 6.41 (d, *J* = 5.4 Hz, 1H, ArH), 7.20-7.76 (m, 7H, ArH), 7.93 (d, *J* = 2.1 Hz, 1H, ArH), 8.49 (d, *J* = 5.4 Hz, 1H, ArH). ^{13}C NMR (75 MHz, $CDCl_3$, 25°C): δ=13.5, 22.8, 27.7, 41.2, 61.7, 66.4, 121.3, 125.3, 130.2, 151.9. Anal. Calcd. For $C_{26}H_{25}N_4O_3Cl$: C, 65.47; H, 5.28; N, 11.75; Found: C, 65.12; H, 4.99; N, 11.89. MS: *m/z* 476.1 [M^+].

5.3.3. Ethyl 4-(4-chlorophenyl)-2-((4-((7-chloroquinolin-4-yl)amino)butylamino)-6-methylpyrimidine-5-carboxylate (**5e**). Yellow solid. Rf: 0.54 (4% MeOH/ethyl acetate). Yield: 85%. m.p. 135ºC. IR (KBr): ν_{max} 1065, 1720, 2930, 3489 cm^{-1}. ^{1}H NMR (300 MHz, $CDCl_3$, 25°C): δ 1.03 (t, *J* = 6.9 Hz, 3H, ester-CH_3), 1.86 (m, 4H, CH_2), 2.46 (s, 3H, C6-CH_3), 3.40 (m, 2H, CH_2), 3.59 (m, 2H, CH_2), 4.07 (q, *J* = 6.0 Hz, 2H, ester-CH_2), 5.50 (br, 1H, NH), 5.78 (br, 1H, NH), 6.36 (d, *J* = 5.7 Hz, 1H, ArH), 7.25-7.37 (m, 5H, ArH), 7.48 (d, *J* = 8.4 Hz, 1H, ArH), 7.96 (d, *J*=7.8 Hz, 1H, ArH), 8.42 (d, *J*=5.7 Hz, 1H, ArH). ^{13}C NMR (75 MHz, $CDCl_3$, 25°C): δ 16.5, 28.8, 30.2, 32.5, 64.1, 101.8, 128.3, 131.3, 132.2, 143.2, 152.4, 161.6, 167.7. Anal. Calcd. For $C_{27}H_{27}N_5O_2Cl_2$: C, 61.84; H, 5.19; N, 13.35; Found: C, 61.57; H, 5.05; N, 13.12. MS: *m/z* 523.1 [M^+].

5.3.4. Ethyl 4-(4-fluorophenyl)-2-((4-((7-chloroquinolin-4-yl)amino)butylamino)-6-methylpyrimidine-5-carboxylate (**5f**). Yellow solid. Rf: 0.34 (4% MeOH/ethyl acetate). Yield: 72%. m.p. 112ºC. IR (KBr): ν_{max} 1156, 1682, 1333, 2928, 3395 cm^{-1}. ^{1}H NMR (300 MHz, $CDCl_3$, 25°C): δ 1.02 (t, *J* = 7.2 Hz, 3H, ester-CH_3), 1.83 (m, 4H, CH_2), 2.46 (s, 3H, C6-CH_3),

3.38 (m, 2H, CH_2), 3.49 (m, 2H, CH_2), 4.08 (q, *J* = 6.0 Hz, 2H, ester-CH_2), 5.40 (br, 1H, NH), 5.74 (br, 1H, NH), 6.37 (d, *J* = 5.4 Hz, 1H, ArH), 7.04-7.55 (m, 6H, ArH), 7.95 (d, *J* = 2.1 Hz, 1H, ArH), 8.47 (d, *J* = 5.7 Hz, 1H, ArH). ^{13}C NMR (75 MHz, $CDCl_3$, 25^{o}C): δ 18.5, 29.6, 31.2, 63.5, 99.8, 126.3, 133.3, 145.2, 153.4, 160.4, 171.7. Anal. Calcd. For$C_{27}H_{27}N_5O_2ClF$: C, 63.84; H, 5.36; N, 13.79; Found: C, 63.76; H, 5.23; N, 13.88. MS: *m/z* 507.1 [M^+].

5.3.5. Ethyl 2-((3-((7-chloroquinolin-4-yl)amino)propylamino)-4-methylpyrimidine-5-carboxylate **(5g)**. White solid. Rf: 0.38 (4% MeOH/ethyl acetate). Yield: 89%. m.p. 143ºC. IR (KBr): ν_{max} 1097, 1702, 2973, 3365 cm^{-1}. ^{1}H NMR (300 MHz, $CDCl_3$, 25^{o}C): δ 1.36 (t, *J* = 7.1 Hz, 3H, ester-CH_3), 1.84 (m, 4H, CH_2), 2.64 (s, 3H, C6-CH_3), 3.40 (d, *J* = 5.4 Hz, 2H, CH_2), 3.58 (m, 2H, CH_2), 4.31 (q, *J* = 7.2 Hz, 2H, ester-CH_2), 5.68 (br, 2H, NH), 6.40 (d, *J* = 5.7 Hz, 1H, ArH), 7.33 (d, *J* = 2.1 Hz, 1H, ArH), 7.84 (d, *J* = 6.0 Hz, 1H, ArH), 7.95 (d, *J* = 2.1 Hz, 1H, ArH), 8.45 (d, *J* = 6.0 Hz, 1H, ArH), 8.70 (s, 1H, ArH). ^{13}C NMR (75 MHz, $CDCl_3$, 25^{o}C): δ 14.3, 40.8, 60.5, 99.1, 125.3, 128.8, 149.0, 151.9. Anal. Calcd. For $C_{21}H_{24}N_5O_2Cl$: C, 60.94; H, 5.84; N, 16.92; Found: C, 61.10; H, 5.75; N, 16.79. MS: *m/z* 413.1 [M^+].

6. Material and Methods

6.1. *In vitro* antimalarial activity assay

The test samples were tested in triplicate on one or two separate occasions against chloroquine sensitive (CQ^S) strain of *P. falciparum* (D10). Continuous *in vitro* cultures of asexual erythrocyte stages of *P. falciparum* were maintained using a modified method of Trager and Jensen [45]. Quantitative assessment of antiplasmodial activity *in vitro* was determined via the parasite lactate dehydrogenase assay using a modified method described by Makler [46]. The test samples were prepared to a 20 mg/ml stock solution in 100% DMSO and sonicated to enhance solubility. Samples were tested as a suspension if not completely dissolved. Stock solutions were stored at -20ºC. Further dilutions were prepared on the day of the experiment. Chloroquine (CQ) was used as the reference drug in all experiments. Test samples were initially tested at three concentrations (10 µg/ml, 5µg/ml and 2.5 µg/ml) to determine the starting concentration for the full dose-response assay. CQ was tested at three concentrations namely 30 ng/ml, 15 ng/ml and 7.5 ng/ml. A full dose-response was performed for all compounds to determine the concentration inhibiting 50% of parasite growth (IC_{50}–value). Test samples were tested at a starting concentration of 10 µg/ml, which was then serially diluted 2-fold in complete

medium to give 10 concentrations; with the lowest concentration being 0.02 μg/ml. The same dilution technique was used for all samples. CQ was tested at a starting concentration of 1000 ng/ml. Several compounds were tested at a starting concentration of 1000 ng/ml. The highest concentration of solvent to which the parasites were exposed to had no measurable effect on the parasite viability (data not shown). The IC_{50}-values were obtained using a non-linear dose-response curve fitting analysis via Graph Pad Prism v.4.0 software.

6.2. Cytotoxicity and antiviral activity assay

Cytotoxicity was determined by exposing different concentrations of samples to vero, HEL, HELA and MDCK cells [29]. The antiviral assays [except anti-human immunodeficiency virus (HIV) assays] were based on inhibition of virus-induced cytopathicity in HEL [herpes simplex virus type 1 (HSV-1), HSV-2 (G), vaccinia virus, and vesicular stomatitis virus], Vero (parainfluenza-3, reovirus-1, Coxsackie B4, and Punta Toro virus), HeLa (vesicular stomatitis virus, Coxsackie virus B4, and respiratory syncytial virus) and MDCK (influenza A (H1N1; H3N2) and B virus) cell cultures. Confluent cell cultures in microtiter 96-well plates were inoculated with 100 cell culture inhibitory dose-50 ($CCID_{50}$) of virus (1 $CCID_{50}$ being the virus dose to infect 50% of the cell cultures) in the presence of varying concentrations of the test compounds. Viral cytopathicity was recorded as soon as it reached completion in the control virus-infected cell cultures that were not treated with the test compounds [29].

Acknowledgements

We gratefully acknowledge financial assistance from CSIR, New Delhi (project 01(2364)/10/EMR-II) and UGC, New Delhi for Special Assistance Programme (SAP). H.K. thanks CSIR, New Delhi for senior research fellowship.

References

[1] R.G.A. Feachem, A.A. Phillips, J. Hwang, C. Cotter, B. Wielgosz, B.M. Greenwood, O. Sabot, M.H. Rodriguez, R.R. Abeyasinghe, T.A. Ghebreyesus, R.W. Snow, Shrinking the malaria map: progress and prospects, Lancet 376 (2010) 1566-1578.

[2] WHO (2010) http://www.who.int/malaria/world_malaria_report_2010/worldmalariareport2010.pdf.

[3] F.-J. Gamo, L.M. Sanz1, J. Vidal, C. Cozar, E. Alvarez, J.-L. Lavandera1, D.E. Vanderwall, D.V.S. Green, V. Kumar, S. Hasan, J.R. Brown, C.E. Peishoff, L.R. Cardon,

J.F.G. -Bustos, Thousands of chemical starting points for antimalarial lead identification, Nature 465 (2010) 305-310.

[4] M. Dondorp, F. Nosten, P. Yi, D. Das, A.P. Phyo, J. Tarning, K.M. Lwin, F. Ariey, W. Hanpithakpong, S.J. Lee, P. Ringwald, K. Silamut, M. Imwong, K. Chotivanich, P. Lim, T. Herdman, S.S. An, S. Yeung, P. Singhasivanon, N.P.J. Day, N. Lindegardh, D. Socheat, N.J. White, Artemisinin resistance in Plasmodium falciparum malaria, N. Engl. J. Med. 361 (2009) 455-469.

[5] M. Schlitzer, Malaria chemotherapeutics part I: History of antimalarial drug development, currently used therapeutics, and drugs in clinical development, Chem. Med. Chem. 2 (2007) 944-986.

[6] B. Meunier, Hybrid molecules with a dual mode of action: Dream or reality? Acc. Chem. Res. 41 (2008) 69−77.

[7] F.W. Muregi, A. Ishih, Next-Generation antimalarial drugs: Hybrid molecules as a new strategy in drug design, Drug Dev. Res. 71 (2010) 20–32.

[8] S. Manohar, S.I. Khan, D.S. Rawat, Synthesis, antimalarial activity and cytotoxicity of 4-aminoquinoline-triazine conjugates, Bioorg. Med. Chem. Lett. 20 (2010) 322−325.

[9] S. Manohar, S.I. Khan, D.S. Rawat, Synthesis of 4-aminoquinoline-1,2,3-triazole and 4-aminoquinoline-1,2,3-triazole-1,3,5-triazine hybrids as potential antimalarial agents, Chem. Biol. Drug Des. 78 (2011) 124−136.

[10] C. Biot, G. Glorian, L.A. Maciejewski, J.S. Brocard, Synthesis and antimalarial activity in vitro and in vivo of a new Ferrocene-Chloroquine analogue, J. Med. Chem. 40 (1997) 3715−3718.

[11] K. Chauhan, M. Sharma, J. Saxena, S.V. Singh, P. Trivedi, K. Srivastava, S.K. Puri, J.K. Saxena, V. Chaturvedi, P.M.S. Chauhan, Synthesis and biological evaluation of a new class of 4-aminoquinoline-rhodanine hybrid as potent anti-infective agents, Eur. J. Med. Chem. 62 (2013) 693-704.

[12] V.R. Solomon, W. Haq, K. Srivastava, S.K. Puri, S.B. Katti, Synthesis and antimalarial activity of side chain modified 4-aminoquinoline derivatives, J. Med. Chem. 50 (2007) 394-398.

[13] E.M. Guantai, K. Ncokazi, T.J. Egan, J. Gut, P.J. Rosenthal, R. Bhampidipati, A. Kopinathan, P.J. Smith, K. Chibale, Enone- and chalcone-chloroquinoline hybrid analogues: In silico guided design, synthesis, antiplasmodial activity, in vitro metabolism, and mechanistic studies, J. Med. Chem. 54 (2011) 3637-3649.

[14] O.D. -Cabaret, F.B. Vical, A. Robert, B. Meunier, Preparation and antimalarial activities of trioxaquines, new modular molecules with a trioxane skeleton linked to a 4-aminoquinoline, Chem. Bio. Chem. 1 (2000) 281−283.

[15] I. Chiyanzu, C. Clarkson, P.J. Smith, J. Lehman, J. Gut, P.J. Rosenthal, K. Chibale, Design, synthesis and anti-plasmodial evaluation in vitro of new 4-aminoquinoline isatin derivatives, Bioorg. Med. Chem. 13 (2005) 3249−3261.

[16] S. Manohar, U.C. Rajesh, S.I. Khan, B.L. Tekwani, D.S. Rawat, Novel 4-aminoquinoline-pyrimidine based hybrids with improved in vitro and in vivo antimalarial activity, ACS Med. Chem. Lett. 3 (2012) 555−559.

[17] S.I. Pretorius, W.J. Breytenbach, C. de Kock, P.J. Smith, D.D. N'Da, Synthesis, characterization and antimalarial activity of quinoline–pyrimidine hybrids, Bioorg. Med. Chem. 13 (2012) 3249−3261.

[18] M. Sharma, V. Chaturvedi, Y.K. Manju, S. Bhatnagar, K. Srivastava, S.K. Puri, P.M. Chauhan, Substituted quinolinyl chalcones and quinolinyl pyrimidines as a new class of anti-infective agents, Eur. J. Med. Chem. 44 (2009) 2081-2091.

[19] R. Ettari, F. Bova, M. Zappala, S. Grasso, N. Micale, Falcipain-2 inhibitors, Med. Res. Rev. 30 (2010) 136-167.

[20] M. Foley, L. Tilley, Quinoline antimalarial: mechanisms of action and resistance, Int. J. Parasitol. 27 (1997) 231-240.

[21] J.X. Kelly, M.J. Smilkstein, R. Brun, W. Sergio, A.R. Cooper, K.D. Lane, A. Janowsky, R.A. Johnson, R.A. Dodean, R. Winter, D.J. Hinrichs, M.K. Riscoe, Discovery of dual function acridones as a new antimalarial chemotype, Nature 459 (2009) 270-273.

[22] N. Hossain, J. Rozenski, E.D. Clercq, P. Herdewijn, Synthesis and antiviral activity of the alpha-analogues of 1,5-Anhydrohexitol nucleosides, J. Org. Chem. 62 (1997) 2442-2447.

[23] K. Singh, K. Singh, B. Wan, S. Franzblau, K. Chibale, J. Balzarini, Facile transformation of 3,4-dihydropyrimidin-2(1H)-ones to pyrimidines in vitro evaluation as inhibitor of

mycobacterium tuberculosis and modulators of cytostatic activity, Eur J. Med. Chem. 46 (2011) 2290-2294.

[24] S. Joseph, J.M. Burke, Optimization of an anti-HIV hairpin ribozyme by in vitro selection, J. Biol. Chem. 268 (1993) 24515-24518.

[25] B.C. Bookser, B.G. Ugarkar, M.C. Matelich, R.H. Lemus, M. Allan, M. Tsuchiya, M. Nakane, A. Nagahisa, J.B. Wiesner, M.D. Erion, Adenosine kinase inhibitors. Synthesis, water solubility, and antinociceptive activity of 5-phenyl-7-(5-deoxy-beta-D-ribofuranosyl) pyrrolo[2,3-d]pyrimidines substituted at C4 with glycinamides and related compounds, J. Med. Chem. 48 (2005) 7808-7820.

[26] S.L. Hargreaves, B.L. Pilkington, S.E. Russell, P.A. Worthington, The synthesis of substituted pyridylpyrimidine fungicides using palladium catalysed cross-coupling reactions, Tetrahedron Lett. 41 (2000) 1653−1656.

[27] M.G. Carlos, R.M. John, D. Charles, Nucleoside analogues and nucleobases in cancer treatment, Lancet Oncol. 3 (2002) 415−424.

[28] D.C. Martyn, A. Nijjar, C.A. Celatka, R. Mazitschek, J.F. Cortese, E. Tyndall, H. Liu, M. M. Fitzgerald, T.J. Shea, S. Danthi, J. Clardy, Synthesis and antiplasmodial activity of novel 2,4-diaminopyrimidines, Bioorg. Med. Chem. Lett. 20 (2010) 228−231.

[29] K. Singh, H. Kaur, K. Chibale, J. Balzarini, S. Little, P.V. Bharatam, 2-aminopyrimidine based 4-aminoquinoline anti-plasmodial agents. Synthesis, biological activity, structure-activity relationship and mode of action studies, Eur. J. Med. Chem. 52 (2012) 82-97.

[30] A. Shaabani, A. Bazgir, F. Teimouri, Ammonium chloride-catalyzed one-pot synthesis of 3,4-dihydropyrimidin-2-(1*H*)-ones under solvent-free conditions, Tetrahedron Lett. 44 (2003) 857–859.

[31] K. Singh, J. Singh, P.K. Deb, H. Singh, An expedient protocol of the Biginelli dihydropyrimidine synthesis using carbonyl equivalents, Tetrahedron 55 (1999) 12873-12880.

[32] A. Puchala, F. Belaj, J. Bergman, C.O. Kappe, On the reaction of 3,4-Dihydropyrimidones with nitric acid. Preparation and X-ray structure analysis of a stable Nitrolic acid, J. Heterocycl. Chem. 38 (2001) 1345-1352.

[33] J.K. Natarajan, J.N. Alumasa, K. Yearick, K.A. Ekoue-Kovi, L.B. Casabianca, A.C. de Dios, C. Wolf, P.D. Roepe, 4-N-, 4-S-, and 4-O-Chloroquine analogues: Influence of side chain length and quinolyl nitrogen pK_a on activity vs chloroquine resistant malaria, J. Med. Chem. 51 (2008) 3466−3479.

[34] E.A. Kouroumalis, J. Koskinas. Treatment of chronic active hepatitis B (CAH B) with chloroquine: a preliminary report, Ann. Acad. Med. 15 (1986) 149-152.

[35] M.K. Kono, A.M. Tatsumi, K. Imai, T. Saito, Kuriyama, H. Shirasawa, Inhibition of human coronavirus 229E infection in human epithelial lung cells (L132) by chloroquine: involvement of p38 MAPK and ERK, Antivir. Res. 77 (2008) 150-152.

[36] W.P. Tsai, P.L. Nara, H.F. Kung, S. Oroszlan, Inhibition of human immunodeficiency virus infectivity by chloroquine, AIDS Res. Hum. Retrovir. 6 (1990) 481-489.

[37] A.K. Singh, G.S. Sidhu, R.M. Friedman, R.K. Maheshwari, Mechanism of enhancement of the antiviral action of interferon against herpes simplex virus-1 by chloroquine, J. Interferon Cytokine. Res. 16 (1996) 725-731.

[38] A. Dorn, R. Stoffel, H. Matile, A. Bubendorf, R. Ridley, Malarial haemozoin/beta-haematin supports haem polymerization in the absence of protein, Nature 374 (1995) 269-271.

[39] P. Gans, A. Sabatini, A. Vacca, Investigation of equilibria in solution. Determination of equilibrium constants with the Hyperquad suite of programmes, Talanta 43 (1996) 1739-1753.

[40] S.R Meshnick, Chloroquine as intercalator: a hypothesis revived, Parasitol Today. 6 (1990) 77-79.

[41] W.D. Wilson, R.L. Jones, Intercalating Drugs: DNA binding and molecular pharmacology, Adv. Pharmacol. Chemoether. 18 (1981) 177-222.

[42] N. Kumari, B.K. Maurya, R.K. Koiri, S.K. Trigun, S. Saripella, M.P. Coogan, L. Mishra, Cytotoxic activity, cell imaging and photocleavage of DNA induced by a Pt(II) cyclophane bearing 1,2 diamino ethane as a terminal ligand, Med. Chem. Com. 2 (2011) 1208-1216.

[43] S.N. Cohen, K.L. Yielding, Spectrophotometric studies of the interaction of chloroquine with deoxyribonucleic acid, J. Biol. Chem. 240 (1965) 3123-3131.

[44] E.T. Mudasir, D.H. Wahyuni, N. Tjahjono, H. Yoshioka, Inoue, Spectroscopic studies on the thermodynamic and thermal denaturation of the CT-DNA binding of methylene blue, Spectrochim. Acta Part A 77 (2010) 528-534.

[45] W. Trager, J.B. Jensen, Human malaria parasite in continuous culture, Science 193 (1976) 673-675.

[46] M.T. Makler, J.M. Ries, J.A. Williams, J.E. Bancroft, R.C. Piper, B.L. Gibbins, D.J. Hinrichs, Parasite lactate dehydrogenase as an assay for *Plasmodium falciparum* drug sensitivity, Am. J. Trop. Med. Hyg. 48 (1993) 739-741.

Captions for Figures

Figure 1. Small molecule antimalarial agents.

Figure 2. Representative designs of 4-aminoquinoline based hybrid drugs showing antimalarial activity (quinoline hybrids with (a) triazine, (b) ferrocene, (c) rhodanine, (d) thiazolidin-4-one, (e) chalcone, (f) trioxane, (g) isatin and (h) pyrimidine).

Figure 3. Quinoline-pyrimidine and quinoline-pyrimidine carboxylate hybrids.

Figure 4. Titration of **5b** with monomeric heme at (a) pH 7.4, (b) pH 5.6.

Figure 5. The 400 MHz ^{1}H spectra of **5b** upon addition of heme (a) 0 mol %, (b) 30 mol %, (c) 50 mol % in 40% DMSO:D_2O\D_2SO_4 (10 µl)) [$\Delta\delta$ for peak: a = 0.002, b = 0.013, c =0.023, d = 0.008, e = 0.007, f = 0.007].

Figure 6. (a) The solution phase mass spectra of **5b** (3.9 µmoles) upon addition of monomeric heme (3.9 µmoles) in 40% DMSO, (b) Proposed binding of heme with **5b** (for optimized structure of **5b**, *see* Figure S2†).

Figure 7. (a) Titration of **5b** with µ-oxo heme at pH 5.8, (b) Job plot of µ-oxoheme complex formation at pH 5.8. x = [**5b**]/[**5b**]+[heme] is the mole fraction of the **5b**, A_0 is the absorbance, when x = 1 and A is the absorbance at respective values of x.

Figure 8. Absorption spectra of **5b** (30 µM) in the presence of increasing CT DNA concentration (4-200 µM); inset show zoom between 280 and 390 nm.

Figure 9. Derivative melting curves of CT DNA, **5b** + CT DNAand **CQ** + CT DNA.

Figure 10. Fluorescence emission spectra (λ_{ex} = 330 nm, λ_{em} = 376 nm) of **5b** (17.1 µM) in buffered CH_3OHupon addition of increasing concentrations of (a) CT DNA (0.5-150 µM), (b) pUC18 DNA (0.02-15 µM).

Captions for Scheme

Scheme 1. Reagents and conditions. (a) NH_4Cl, 100^{o}C, 3 h, (b) 60% HNO_3, 0^{o}C, 30 minutes, (c) $POCl_3$, 105^{o}C, 45 minutes, (d) THF /MeCN, K_2CO_3, 70^{o}C ,48 h.

Captions for Tables

Table 1. *In vitro* antimalarial activity of compounds **5a-g** against *P. falciparum* (CQ^S) D10 strain and (CQ^R) Dd2 strain for n=3 (n=number of replicates).

Table 2. Anti-Feline Corona Virus (FIPV) and anti-Feline Herpes Virus activity and cytotoxicity in Crandell-Rees Feline Kidney (CRFK) cell cultures.

Table 3.Binding constant (log K) of **5b** and CQ with heme and DNA.

- New hybrids of 4-aminoquinoline and pyrimidine were synthesized efficaciously.
- nM range antiplasmodial activity.
- Activity against both CQ^S and CQR strains of Plasmodium falciparum.
- Effective binding to heme as well as AT rich pUC18 DNA.

Table 1

Compound	Structure	Yield (%)	D10 IC_{50} (nM)[a,b]	Dd2 IC_{50} (nM)[b,c]	ClogP[d]	CC_{50}(μM)[e,f]	SI[g]
5a	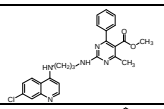	86	659	542	6.71	1.7	3.13
5b	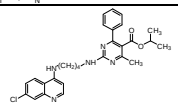	83	156	153	7.66	0.6	3.92
5c	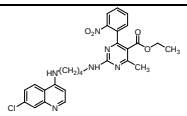	75	1461	nd	7.10	0.8	-
5d	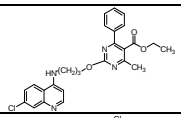	90	478	483	7.24	21.1	43.6
5e	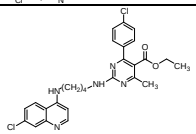	85	1926	nd	8.07	2.2	-
5f	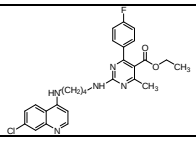	72	2759	nd	7.50	11.4	-
5g	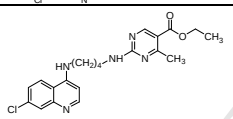	89[h]	211	336	5.25	10.3	30.65
6a[i]	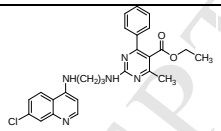	-	202[j]	26.1[k]	6.82	0.8	15.33
6b[i]	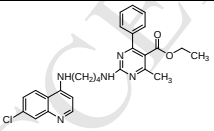	-	247.5[j]	52.2[k]	7.35	0.9	34.41
6c[i]	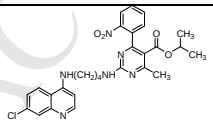	-	18.2[j]	3.6[k]	7.3	2.3	638
CQ			35	221.9	-	-	-
ASN			-	31.2	-	-	-
MMV390048			-	17.8			

[a]CQ sensitive strain;.[b]Data represents the mean of three independent experiment; [c]CQ resistant strain.; [d]calculated from Chem draw Ultra 11.0; [e]determined on Madin Darby canine kidney (MDCK)cells; [f] 50% cytotoxic concentration, as determined by measuring the cell viability with the colorimetric formazan- based MTS assay (reference drugs used: Oseltamivir carboxylate CC_{50}/MIC >100, Ribavirin CC_{50}/MIC >100, Amantadine CC_{50}/MIC >200 and Rimantadine CC_{50}/MIC >200); [g] Selectivity Index(S.I.) is calculated as CC_{50}/ IC_{50} (Dd2 Strain) ratio; [h]prepared by usingperhydro 1,3-oxazine(1.5 equiv.) as formaldehyde equivalent (CH_3CN:TFA(10:1, v/v) solution/70 °C.[31] [i] see text reference 29; [j] 3D7 strain used; [k] K1 strain used.

Table 2

Compound	CC_{50}(µM)[a]	EC_{50} (µM) [b]	
		Feline Corona Virus (FIPV)	Feline Herpes Virus
5a	25.1	1.1	>20
5b	50.6	>20	>20
5c	>100	9.0	>100
5d	>100	>100	>100
5e	>100	>100	>100
5f	>100	>100	>100
5g	>100	>100	>100
HHA (µg/ml)	>100	32.5	2.9
UDA (µg/ml)	63.2	1.6	1.0
Ganciclovir	>100	>100	4.1

[a]50% Cytotoxic concentration as determined by measuring the cell viability with the colorimetric formazon-based MTS assay; [b]50% Effective concentration or concentration producing 50% inhibition of virus-induced cytopathic effect as determined by measuring the cell viability with the colorimetric formazon-based MTS assay.

Table 3

Compound	Monomeric heme log $K \pm \sigma$		μ-oxoheme log $K \pm \sigma$	CT DNA log K	pUC18 DNA log K
	pH 5.6	pH 7.4	pH 5.8		
5b[a]	4.58 ± 0.042	4.96 ± 0.029	5.72 ± 0.025	5.76	5.73
CQ	4.65±0.052	5.15 ± 0.176	5.58 ± 0.006	ND	ND
Stoichiometry	1:1		1:1	ND	

[a] *calculated from HypSpec software.*

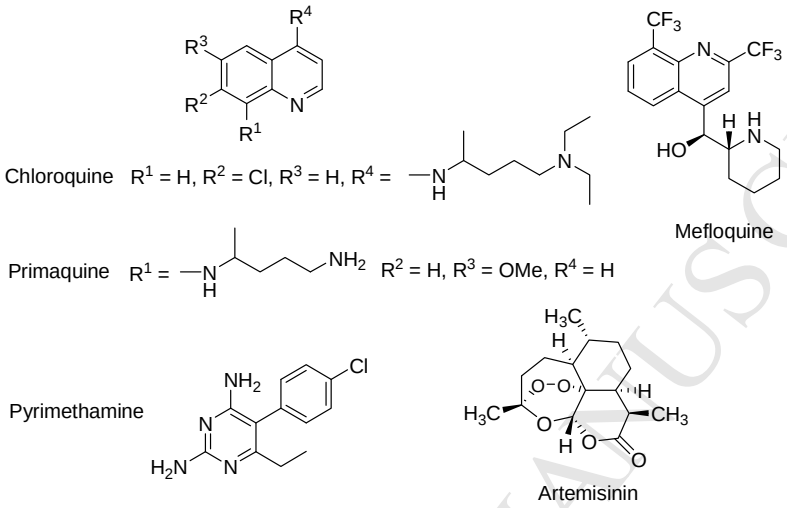

Figure 1

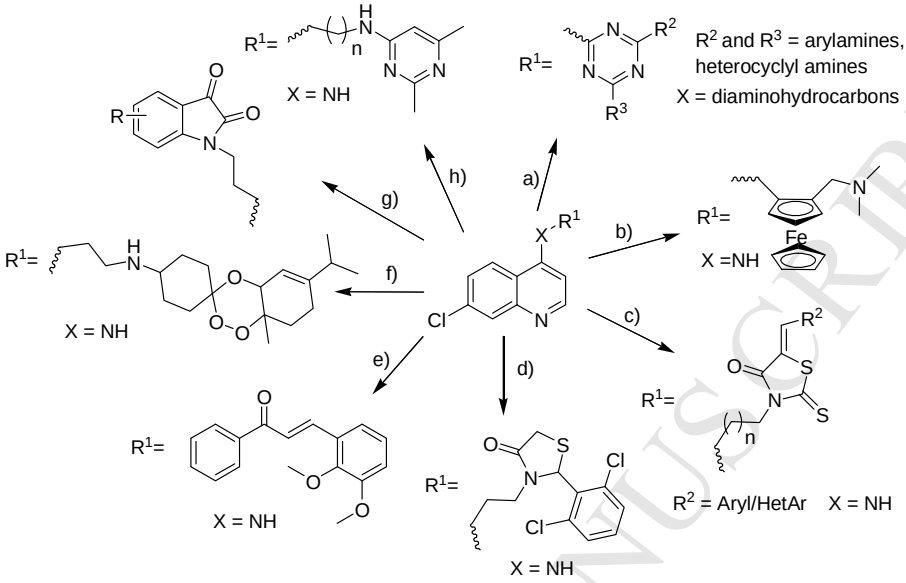

Figure 2

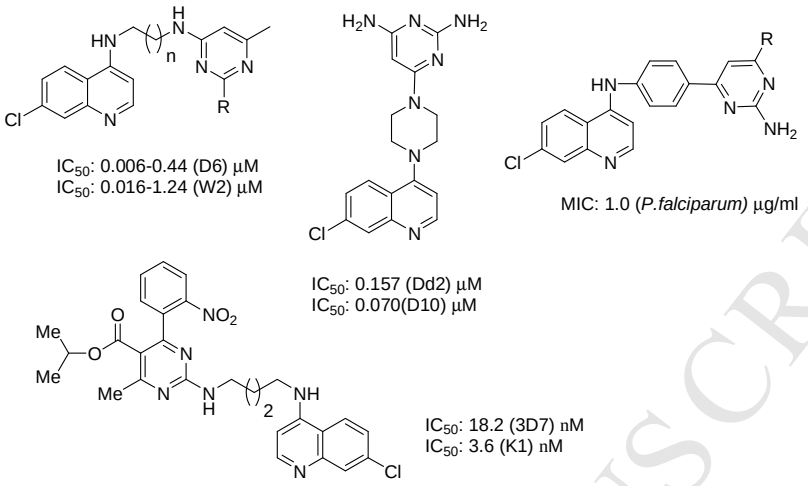

Figure 3

(a)

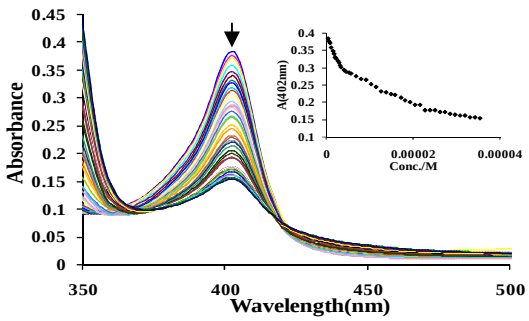

(b)

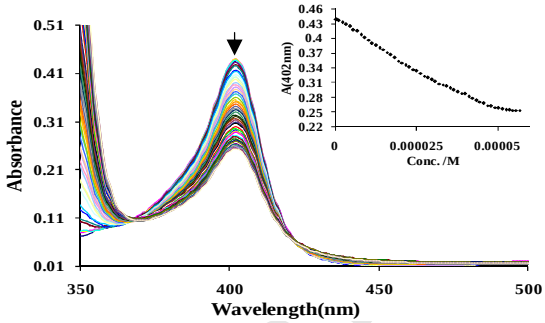

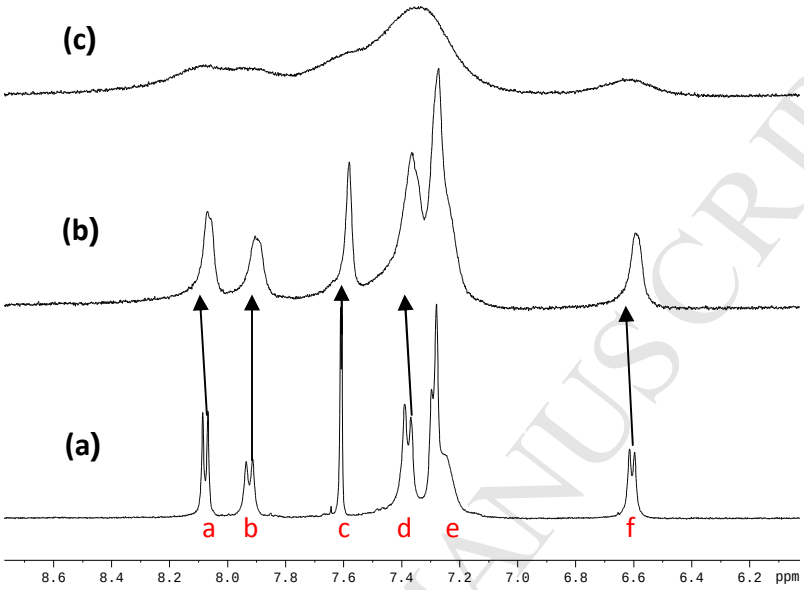

Figure 5

(a)

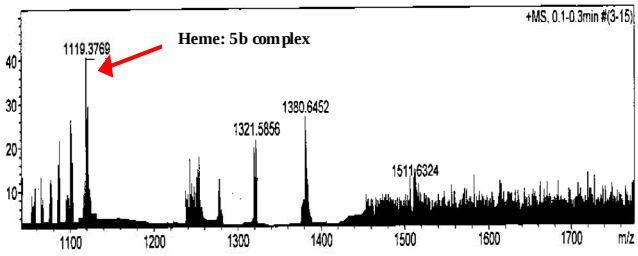

(b)

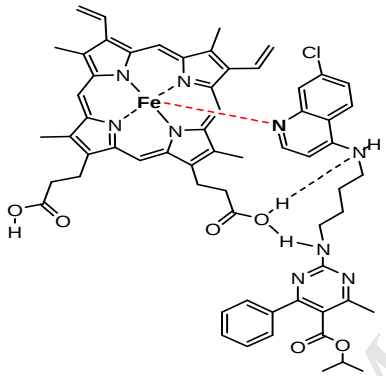

Figure 6

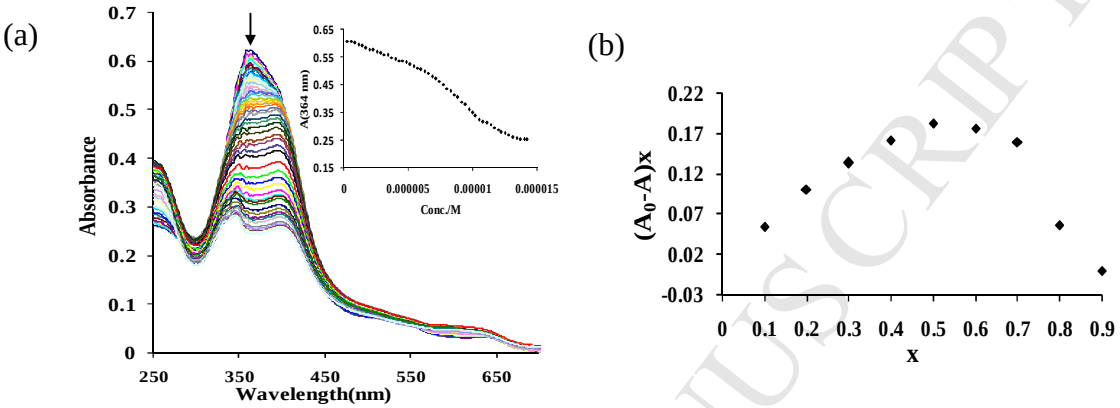

Figure 7

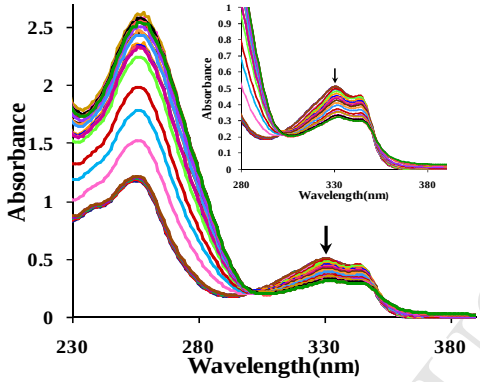

Figure 8

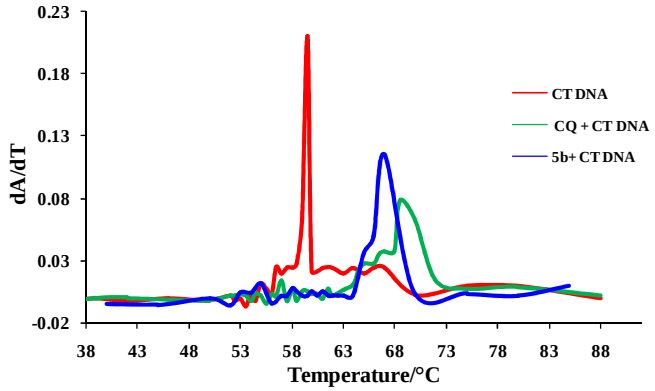

Figure 9

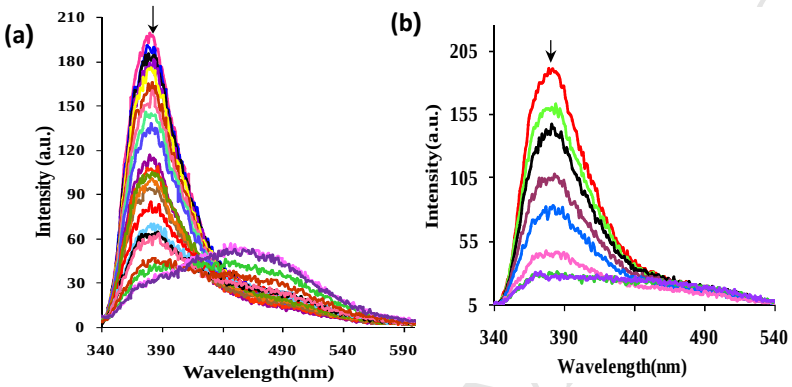

Figure 10

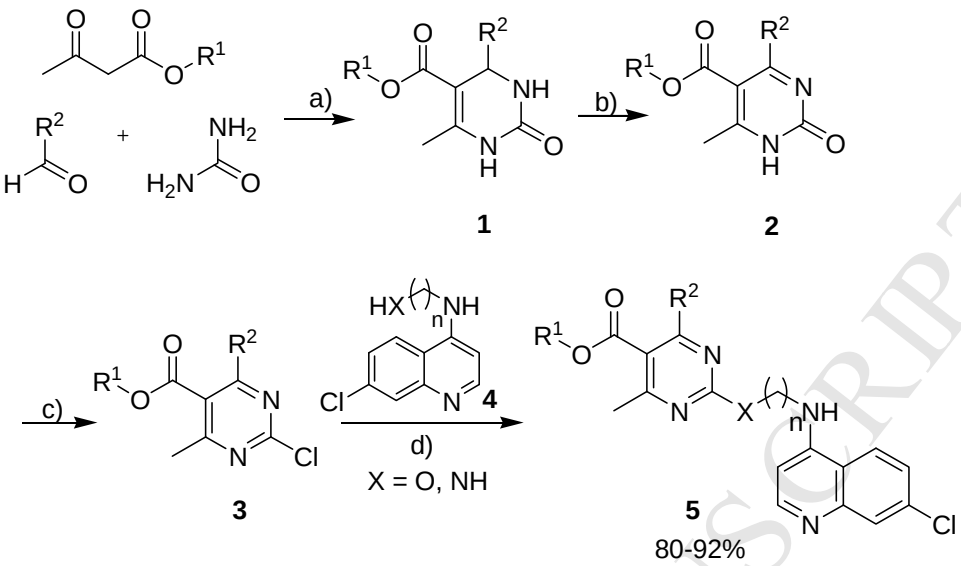

Scheme 1

SUPPLEMENTARY MATERIALS

Synthesis of 4-aminoquinoline–pyrimidine hybrids as potent antimalarials and their mode of action studies

Kamaljit Singh, Hardeep Kaur, Kelly Chibale and Jan Balzarini

Table of contents:

S1. Experimental

1. Heme Binding Studies:

(a) Monomeric Heme: Hemin stock solution (1.2 mM) was prepared by dissolving (7.8 mg) hemin chloride in 10 ml AR grade DMSO. Then, 2.4 µM working solution were prepared daily by mixing 20µL hemin stock solution with 4 ml DMSO and 1ml 0.2 M HEPES buffer (pH 7.4) and making it up to 10ml with double distilled deionized water. Stock solution of drug (2 mM) was prepared in AR grade DMSO and was used for titration experiment. Heme (2.4 µM) was titrated with increasing concentrations (0- 25 µM) of drug. Following each addition sample was mixed & absorbance was recorded at 402 nm. Solution of drug and of Fe(III)PPIX at an apparent pH of 5.6 was prepared in exactly same manner, except that 2-[N-morpholino]ethanesulphonate (MES) buffer (pH 5.4) was substituted for HEPES buffer.[1]

(b) µ-oxodimericheme: Stock solution (1 mM) of heme was prepared by dissolving hemin chloride in 0.1 M NaOH. Solution was sonicated for 30 min to ensure complete dissolution. Then, heme stock solution was diluted to 10µM in Phosphate buffer (20mM, pH 5.8). Stock solution of drug (2 mM) was prepared in AR grade DMSO .Titration with drug were performed by successive addition of aliquots of stock solution of drug (0-14 µM) to 10 µM heme solution & absorbance at 362 nm was recorded.[2] The association constants for both monomeric and µ-oxodimericheme were determined by using Hyp Spec.

(c) Binding Stoichiometry: Binding Stoichiometries of drug with monomeric & µ-oxodimericheme were monitored by UV-visible spectrophotometry using Job method of continuous variation.[3] The concentration of drug &heme in solution was kept constant and change in absorbance at 402 nm (monomeric) / 362 nm (dimeric) was monitored as a function of the mole fraction.

(d) Ferriprotoporphyrin IX Biomineralisation Inhibition test (FBIT): 96 well plate containing mixture of 50 µL of 0.5 mg\ ml of hemin chloride dissolved in DMSO, 100 µL of 0.5 M sodium acetate buffer (pH 4.4) and 50µL of different concentrations of drug solution

[1] T.J. Egan, W.W. Mavusu, D.C. Ross, H.M. Marques, J. Inorg. Bio chem. 68 (1997) 137.

[2] J.X. Kelly, R. Winter, M. Riscoe, D.H. Peyton, J. Inorg. Biochem. 86 (2001) 617.

[3] C.Y. Huang, *Methods Enzymol.* 87 *(*1982) 509-525.

or 50 µL of solvent (control),was incubated at 37°C for 24 hrs. The plate was centrifuged at 4500 rpm for 3 min, and supernatant was discarded. The remaining pellet was resuspended with 200 µL of DMSO to eliminate unreacted hemin.Then, the plate was centrifuged again and supernatant similarly discarded. The precipitate was dissolved in 150 µL of 0.1 N NaOH& absorbance was read at 405 nm.[4,5] The percentage of inhibition of Ferriprotoporphyrin IX Biomineralisation was calculated using formula:

Inhibition (**%) =** 100 X {[(Abs of control) - (Abs of drug)]/ (Abs of control)}.

2. DNA Binding Studies:

(a) Preparation of Drug solution: Stock solution of drug (2 mM) was prepared by dissolving drug in AR grade methanol. The DNA binding experiments were carried out by making dilution of drug stock with 1:3 TE buffer/methanol.

(b) Preparation of CT DNA solution: Stock solution of DNA was prepared by dissolving DNA pellet in TE buffer (10 mMTris-HCl, 0.1Mm EDTA, pH 7.4). The DNA concentration was estimated from its absorbance intensity at 260 nm with a known molar absorption coefficient value of 6600 dm^3 mol^{-1} cm^{-1}.The purity of DNA was established from ratio of absorbance intensity at 260 nm and at 280 nm. In our case, ratio is 1.8 suggesting that DNA is free from protein.

(c) UV-Spectrophotometry titration: The titration experiment was performed by varying the concentration of CT DNA (4-200 µM) and keeping the drug concentration constant (30 µM). All the UV spectra were recorded after equilibration of solution for 5 min.

(d) Spectrofluorometry titration: The steady state fluorescence experiments were carried out on Cary Eclipse Spectrofluorometerat ambient temperature. A slit width of 5 nm was used with λ_{ex}= 320 nm andλ_{em} = 380 nm. The titration experiment was accomplished by varying the concentration of DNA in cuvette [(0.5-150 µM) for CT

[4]E. Deharo, R. Garcia, Exp. parasitol. 100 (2002) 252.
[5] F. Rodriguez, I. Rozas, J. Med. Chem. 51 (2008) 909.

DNA and (0.02-15 µM) for pUC DNA)] and keeping the drug concentration constant (17.1 µM).The binding constants were calculated by using Hyp Spec.

(e) DNA thermal denaturation: DNA melting experiment were carried out by monitoring the absorbance of CT DNA (151 µM NP) at 260 nm at various temperature in the presence and absence of drug in a 5:1 ratio of the DNA and drug with a ramp rate of 0.5^{o}C/ min in a 40% DMSO/ TE buffer (pH 7.4) with 0.5 mMNaCl on a Shimatzu Spectrophotometer equipped with a Peltier thermo regulator. The Thermal melting temperature was calculated by plotting dA/dTvs temperature.[6]

3. **Energy minimization of 5b:** The theoretical calculations were carried out by using the Gaussian 09 suite of programs. The molecular geometry of **5b** was optimized by DFT/B3LYP[7] in which 6-31G basis set was used for C and H and 6-311G** basis set was used for the donor atoms (N, Cl, and O).

[6]N.I. Wenzel, N. Chavain, Y. Wang, W. Friebolin, Maes, B. Pradines, M. Lanzer, V. Yardley, R. Brun, C. Herold-Mende, C. Biot, K. Toth, E. Davioud-Charvet, J. Med. Chem. 53 (2010) 3214−3226.

[7]L. J. Bartolottiand, and K. Fluchick, *Reviews in Computational Chemistry* K. B.; Lipkowitz, B. D. Boyd, Eds., VCH, New York, 1996, **7**, 187.

Table S1. Cytotoxicity and antiviral activity of 5a-g

		Compounds	5a	5b	5c	5d	5e	5f	5g	Ganciclovir	Cidofovir	Acyclovir	Brivudin	DS-5000 µg/ml	(S)-DHPA	Ribavirin	Oseltamivir carboxylate	Amantadine	Rimantadine
		Cytomegalovirus																	
HEL cells	EC_{50} (µM)[a]	AD-169 strain	10.94	>4	>4	2	>4	>4	>20	7.87	0.86								
		Davis strain	15.3	>4	>4	2.53	>4	>4	>20	5.98	1.84								
	MCC (µM)[b]		20	20	20	4	20	20	100	>350	317								
		Varcella-zoster Virus																	
HEL cells	EC_{50} (µM)[c]	TK^+VZV(OKA)	>4	4	>4	>4	>4	>4	>20			0.026	3.82						
		TK^-VZV (07-1)	>4	>4	>4	>4	>4	>4	>20			143.6	144.9						
	MCC (µM)[b]		20	20	20	20	20	20	100			300	>440						
		Herpes Simplex Virus-1 (KOS)	>20	>4	>4	>100	>20	>100	>100	0.03	2	0.4	0.04						
		Herpes Simplex Virus-2 (G)	>20	>4	>4	>100	>20	>100	>100	0.03	2	0.2	146						
HEL cells	EC_{50} (µM)[d]	Vaccinia virus	>20	>4	>4	>100	>20	>100	>100	>100	17	>250	5						
		Vesicular Stomatitis Virus	>20	>4	>4	>100	>20	>100	>100	>100	>250	>250	>250						
		Herpes Simplex Virus-1 TK-KOS ACV	>20	>4	>4	>100	>20	>100	>100	4	2	112	250						
	MCC (µM)[b]		≥20	20	20	>100	100	≥100	>100	>100	>250	>250	>250						
		Vesicular Stomatitis virus	>20	>100	>20	>100	>100	>100	>20					100	>250	29			
HeLA cells	EC_{50} (µM)[d]	Coxsackie virus B4	>20	>100	>20	>100	>100	>100	>20					45	>250	112			
		Respiratory Syncytial virus	>20	>100	>20	>100	>100	>100	>20					0.7	>250	5			
	MCC (µM)[b]		100	>100	100	>100	>100	>100	100					>100	>250	>250			
		Parainfluenza-3	>4	>4	>0.8	>20	>0.8	>4	>20					>100	146	146			
		Reovirus-1	>4	>4	>0.8	>20	>0.8	>4	>20					>100	>250	>250			
Vero cells	EC_{50} (µM)[d]	Sindbis virus	>4	>4	>0.8	>20	>0.8	>4	>20					100	>250	>250			
		Coxsackie virus B4	>4	>4	>0.8	>20	>0.8	>4	>20					>100	>250	>250			
		Punts virus B4	>4	>4	>0.8	>20	>0.8	>4	>20					>50	>250	126			
	MCC (µM)[b]		20	20	4	100	4	20	100					>100	>250	>250			
		Influenza A H1N1sub type	>0.16[e]	>0.16[e]	>0.16[e]	>4[e]	>0.8[e]	>4[e]	>4[e]							2[e]	0.03[e]	18[e]	4[e]
			>0.16[f]	>0.16[f]	>0.16[f]	>4[f]	>0.8[f]	>4[f]	>4[f]							2.5[f]	0.09[f]	17[f]	6.4[f]
MDCK cells	EC_{50} (µM)[d]	Influenza A H3N3 sub type	>0.16[e]	>0.16[e]	>0.16[e]	>4[e]	>0.8[e]	>4[e]	>4[e]							2[e]	0.3[e]	0.4[e]	0.05[e]
			>0.16[f]	>0.16[f]	>0.16[f]	>4[f]	>0.8[f]	>4[f]	>4[f]							1.1[f]	0.02[f]	0.3[f]	0.01[f]
			>0.16[e]	>0.16[e]	>0.16[e]	>4[e]	>0.8[e]	>4[e]	>4[e]							2[e]	2[e]	>200[e]	>200[e]
		Influenza B	>0.16[f]	>0.16[f]	>0.16[f]	>4[f]	>0.8[f]	>4[f]	>4[f]							2.8[f]	1.1[f]	>200[f]	>200[f]
	MCC (µM)[b]		0.8	0.8	0.8	20	≥0.8	20	≥4							>100	>100	>200	>200

[a] *Effective concentration required to reduce virus plaque formation by 50%. Virus input was 100 plaque forming units (PFU);* [b] *Minimum cytotoxic concentration that causes a microscopically detectable alteration of cell morphology;* [c] *Effective concentration required to reduce virus plaque formation by 50%. Virus input was 20 plaque forming units (PFU);* [d] *Required to reduce virus-induced cytopathogenicity by 50 % ;* [e] *visual CPE Score;* [f] *MTS.*

ACCEPTED MANUSCRIPT

Table S2.β-Hematin inhibition of **5a-g**.

Compound	% Inhibition[a]	Compound	% Inhibition[a]
5a	46	**5e**	56
5b	72	**5f**	59
5c	49	**5g**	58
5d	87	**CQ**[c]	98

[a]*The percentage inhibition at 1mg/ml (highest concentration tested).*

Table S3. Melting temperatures of CT DNA and CT DNA in the presence of **5b** and **CQ**.

S. No.	Composition	Melting temperature/T_m (^oC)	ΔT_m(^oC)
1.	CT DNA	59.5	-
2.	CT DNA+**5b**	67	7.5
3.	CT DNA + CQ	68.5	9

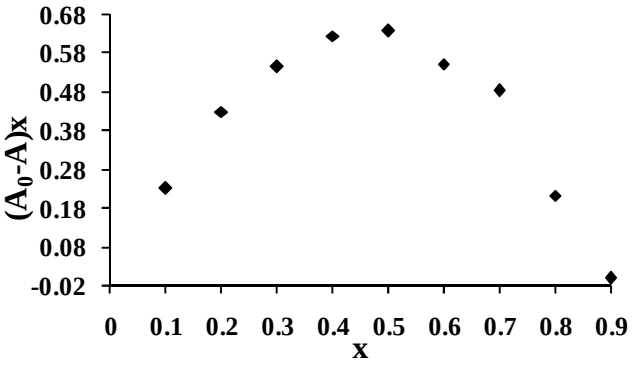

FigureS1. Job plot of monomeric heme complex formation at pH7.4; x = [**5b**]/[**5b**]+[heme] is the mole fraction of the **5b**, A_0 is the absorbance, when x = 1 and A is the absorbance at respective values of x.

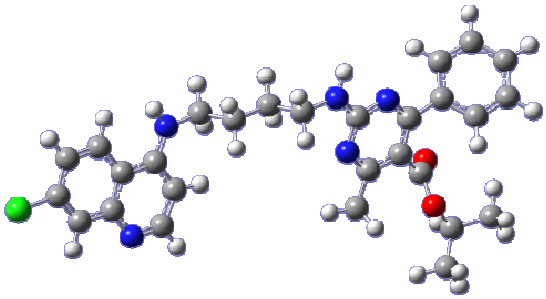

Energy = -1969.8677 a.u

Figure S2. Optimized structure of **5b** using Gaussian 09 program.